General information

1-1   The maximum decay heats specified in the Certificate of Approval (CA) and in the SAR are consistent.
        In the BAM Design Examination Certificate Tables 4 and 5 only parts of this specification are summarized. But both tables additionally refer to Table 25 of the examination certificate which specifies the maximum decay heats correctly.
        Therefore in our opinion there is no inconsistency between the different documents.
        Besides this the design examination certificate is an official document issued by BAM and NCS is not allowed to revise this document.

1-2   In the German version of the CA and in chapter 3 of the SAR the definition for these two parts of the containment are identical with:
        - "Flansch des Bodenstopfens" and
        - "Ausstoßstopfendeckel"
        The different naming of the parts in the translation of the documents (CA and SAR) occurs because different people translated the documents.
        The inconsistency will be remedied at the next opportunity. The correct translation should be "bottom lid" and "discharge plug lid".
        Concerning the mass differences the value of 19650 kg in the CA corresponds to the cask without shock absorbers. In the SAR this value is specified with 19560 kg.
        The value of 22660 kg in the CA is the maximum gross weight and corresponds in the SAR to 22360 kg.
        The small discrepancy between the values is explained by the fact that the values in the SAR are calculated values by the CAD program whereas the final values in the CA are based on actual weight measurements of the manufactured serial cask.

Structural

2-1   (a)
        The 1:3 test specimen was manufactured according to the same specification SB-02-01 as the serial cask. This includes the tests after manufacture as specified in the construction control plan in Annex 3 of the specification. In a final step an acceptance certificate was prepared by the independent expert of BAM which summarizes the results of the inspections and also mentions the non-conformities.

        (b)
        In chapter 4.4.2 of the SAR it is stated that during the water spray test no intake of water can occur because of the metallic or painted surface. Therefore no water spray test was performed. The time interval between the conclusion of the water spray test and the succeeding test is not relevant.

        (c)
        The water leakage test is discussed in the SAR chapter 4.5.6.3 (called water immersion test there). It is not explicitly mentioned that the tests takes place after the mechanical and thermal tests. But the condition of the parts of the containment system is not changed by the mechanical and thermal tests.
        Therefore it is irrelevant if the leakage test is performed before or after the other tests.
        During the fire test the melting plugs in the outer shell melt, causing water

leaking into the thermal insulation during the water leakage test. However in the criticality calculations it is shown that maximum reactivity occurs for a complete dry thermal insulation and that the presence of water reduces the reactivity.

(d)
See 2-1 (c)

(e)
The impact test according to para 737 is only applicable for packages transported by air. Since the NCS 45 is not licensed for air transport this test has not to be looked at.

2-2   The wood types used in the shock absorbers are balsa and spruce, with spruce wood only as a ring at the front sides of the shock absorbers.
Report B-TA-3991-Rev. 2 was prepared in an early design stage (2005) using pine wood instead of later spruce. This report was prepared to find the most unfavourable angle for the slap-down drop test. Because the spruce/pine wood is only positioned at the front sides and is not affected by the slap-down drop the assumed kind of wood has no influence on the results of this report. Consequently there was no need to revise this report when the material was changed.

2-3   At the time report B-TA-3991-Rev. 2 was prepared only results of old static wood tests of BAM from 1978 were available. Since for the results of the report (determination of the slap-down drop angle) only the values for the longitudinal stressed Balsa wood in the radial area of the shock absorbers are of relevance this graph is included in the following.
As stated in chapter 7.3 these values of the graph were conservatively increased (by approx. a factor of 1.5) to take into regard uncertainties of the wood behavior.
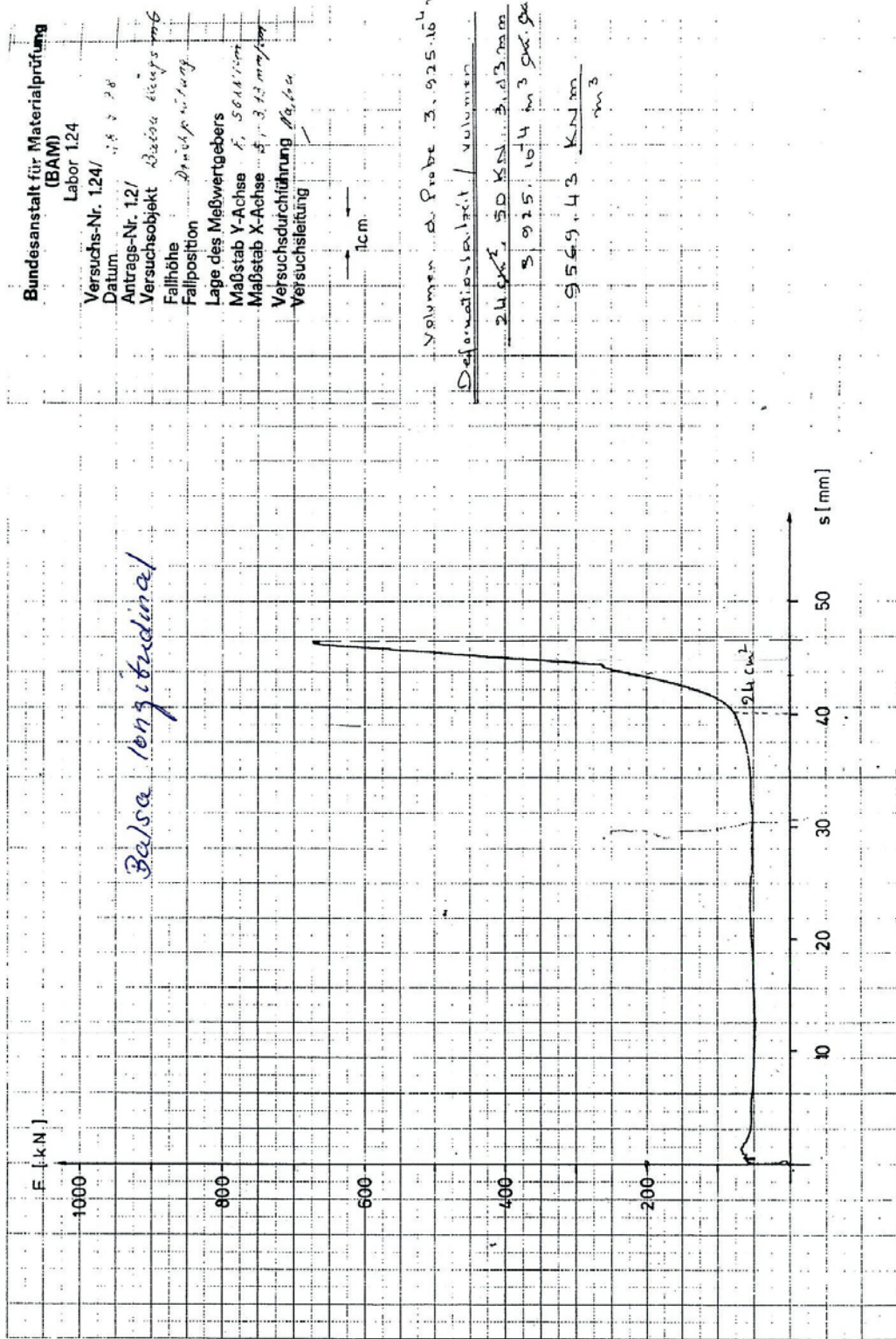
Deformation graph Balsa wood longitudinal with casing

2-4   Data in table 4-30 were compiled from attachment 4.5 SAR: Calculation of static and dynamic tests with wood specimen. These tests were performed by BAM with specimen of the used wood of the shock absorbers. These data are not published in [Niemz 1993].

2-5   The Young's modulus of the plaster is only used in the report B-TA-3991 Rev. 2. A small value was chosen in order to minimize the effect of the plaster onto the deformation.
        The density of 1890 kg/m3 is used for the plaster in the shielding analysis. In the thermal analysis a value of 2060 kg/m3 is used based on the test results documented in the ASTM data sheets. The lower density was used for the shielding analysis as conservative assumption.

2-6   This limiting temperature of 573 °C was used because at this the $\beta \rightarrow \alpha$ Sio2 transformation (quartz inversion) takes place (see excerpt from Literature below) As stated on page 22 of chapter 5 the heat conductivity and density are taken from [FIW 2007] (already sent).
        The specific heat capacity is given for the calculations for normal conditions of transport in Table 5-5 with 1000 J/kg K. This consist of a value of 880 J/kg K given in [VDI 1988] (see excerpt below) for concrete taking into regard additional approx. 4% water with 4180 J/kg K. But the value of 1000 J/kg K is not relevant because in the steady state calculation this value is not used. For the transient accident calculations 880 J/kg K is used (see chapter 5.7.2.4).

SCHRIFTENREIHE SPEZIALBETONE BAND 4

Massenbeton
Helmut Kollo

Feuerbeton
Eberhard Lang

VBT GmbH
Verlag Bau+Technik

Excerpt Literature [Kollo 2001]

und mit Hochofenstückschlacken nicht über 1200 °C belastet werden. Letzteres ist der Maximalwert für besonders günstig zusammengesetzte Hochofenstückschlacken.

Als Zuschlag lassen sich am besten solche Mineralstoffe verwenden, deren Wärmedehnung nicht zu hoch ist und die unter der thermischen Belastung keine Modifikationsumwandlungen aufweisen. Die Wärmedehnung ist eine nichtlineare Funktion der Temperatur, auch schon bei relativ niedrigen Temperaturen. Die Zuschlagart – und hierbei insbesondere die der Grobzuschläge – ist die Haupteinflussgröße auf die Wärmedehnung [24, 25, 26]. Die Verwendung von quarzitischen Zuschlägen ist aufgrund ihrer hohen Wärmedehnung und der $\beta \rightarrow \alpha$ SiO_2 Umwandlung bei 573 °C (Quarzsprung) nur sehr begrenzt möglich. Die Umwandlung von β-Quarz mit einer Dichte von 2.65 kg/dm³ in α-Quarz mit einer Dichte von nur 2.52 kg/dm³ hat zwangsläufig eine Volumenzunahme zur

Folge. Dies führt im Mörtel und Beton vor allem bei mehrmaligem Über- und Unterschreiten der Umwandlungstemperatur zu starken Gefügestörungen. Die Umwandlung des α-Quarzes in α-Tridymit bei 870 °C hat eine weitere Verringerung der Dichte auf 2.26 kg/dm³ zur Folge. Kalksteine weisen eine niedrige und relativ gleichmäßige Wärmedehnung auf. Im Temperaturbereich zwischen 600 °C und 900 °C erfolgt jedoch die Entsäuerung des Kalksteins ($CaCO_3 \rightarrow CaO + CO_2$). Dabei werden 44 M.-% des Kalksteins in Form von CO_2 freigesetzt. Dichte, feinkristalline Kalksteine weisen eine geringere Dehnung als grobkristalline auf.

Die wichtigsten Gesteinseigenschaften von Normalzuschlag vermittelt Tafel 4.3 [27].

Den Einfluss der Zuschläge auf die thermische Dehnung im Zementmörtel und im Beton zeigen die Bilder 4.3 und 4.4. Im Gegensatz zu den grobkristallinen Quarziten hat das Basaltgestein einen feinkristallinen Aufbau

93

| De 2 | Stoffwerte von Feststoffen und Isolierstoffen | | | | | VDI-Wärmeatlas 5. Auflage 1988 |

Tabelle 1.
Wärmetechnische Stoffwerte von Metallen und ihren Legierungen. Nach [1]

ϑ Celsius-Temperatur
ρ Dichte
c spezifische Wärmekapazität
λ Wärmeleitfähigkeit
a Temperaturleitfähigkeit

Stoff	ϑ °C	ρ 10^3 kg/m³	c J/kg K	λ W/m K	a 10^{-6} m²/s	Schmelz-temperatur °C
Aluminium (99,5 %)	20	2,70	920	221	88,89	659
Duraluminium	20	2,80	910	146	57,23	520 bis 650
Silumin	20	2,70	900	160	65,56	570
Antimon	20	6,69	210	21	15,00	630
Blei	20	11,34	130	35	23,61	327
Cadmium	20	8,64	234	9,6	4,72	321
Chrom	20	7,10	500	86	24,17	1800
Eisen	20	7,86	465	67	18,33	1530
Grauguß	20	7,1 bis 7,3	545	42 bis 63		1152 bis 1350
Stahl 0,2 % C	20	7,85	460	50	13,89	1500
Stahl 0,6 % C	20	7,84	460	46	12,78	1470
V2A 18 % Cr, 8 % Ni	20	7,88	500	21	5,28	1400
Invarstahl 36 % Ni	20	8,13	500	16,3	4,17	1450
Gold	20	19,30	125	314	130,57	1063
Kupfer (rein)	20	8,90	390	393	113,34	1083
Magnesium	20	1,74	1010	171	97,23	180
Gelbtombak MS 72	20	8,56	390	92	27,79	920
Rottombak MS 90	20	8,80	390	110	31,95	1030
Konstantan	20	8,90	410	22,5	6,11	
Nickel	20	8,80	460	58,5	14,44	1452
Monelmetall (67 % Ni, 28 % Cu, 5 % Fe+Mn+Si+C)	20	8,58	500	25	5,83	1315 bis 1350
Platin	20	21,40	167	71	13,06	1774
Quecksilber	20	13,60	138	10,5	5,56	−38,9
Silber	20	10,5	238	458	183,35	960
Tantal	20	16,6	138	54,5	11,94	3000
Wismut	20	9,8	125	9,6	7,78	271
Wolfram	20	19,3	142	197	7,22	3380
Zink	20	7,14	376	109	40,84	419
Zinn	20	7,28	230	63	37,50	232

Tabelle 2.
Wärmetechnische Stoffwerte von anorganischen und organischen Stoffen. Nach [2]

	ϑ °C	ρ 10^3 kg/m³	c J/kg K	λ W/m K		a 10^{-6} m²/s
Anorganische Stoffe						
Silicastein	100	1,7 bis 2,0	−	0,81	bis 1,34	−
Schamottestein	100	1,7 bis 2,0	835	0,46	bis 1,16	0,3334 bis 0,6945
Kesselstein	100	0,3 bis 2,7	−	0,081	bis 2,2	−
Beton	20	1,9 bis 2,3	880	0,8	bis 1,4	0,5000 bis 0,6945
Ziegelstein, trocken	20	1,6 bis 1,8	835	0,38	bis 0,52	0,2778 bis 0,3611
Verputz	20	1,7	−	0,79		−
Erdreich, grobkiesig	20	2,0	1840	0,52		0,1444
Sandboden	20	1,6	−	1,07		−
Tonboden	20	1,5	880	1,28		1,000
Sandstein	20	2,2 bis 2,3	710	1,63	bis 2,10	1,0556 bis 1,2779
Marmor	20	2,5 bis 2,7	810	2,8		1,3890
Schnee (Reif)	0	0,2	−	0,15		−
Schnee (frisch)	0	0,1	2090	0,11		0,5278
Eis	0	0,92	1930	2,2		1,2501
Organische Stoffe						
Bakelit	20	1,27	1600	0,23		0,1139
Gummi	20	1,10	−	0,13	bis 0,23	−
Leder	20	1,00	−	0,15		−
Hochdruck-Polyethylen	20	0,92	2150	0,35		0,1778
Niederdruck-Polyethylen	20	0,95	1800	0,45		0,2667
Polypropylen	20	0,91	1700	0,22		0,1417
Polystyrol	20	1,05	1300	0,17		0,1250
Polymethylmethacrylat	20	1,18	1300	0,19		0,1250
Polyvinylchlorid	20	1,39	980	0,17		0,1250
6-Polyamid	20	1,13	1900	0,27		0,1250
6,6-Polyamid	20	1,14	1900	0,25		0,1167
Polyethylenterephthalat	20	1,38	1100	0,28		0,1833
Polytetrafluorethylen	20	2,20	1000	0,23	bis 0,47	0,1055 bis 0,2139
Polytrifluorethylen	20	2,10	920	0,11	bis 0,23	0,0583 bis 0,1194
Polyurethan	20	1,20	1900	0,36		0,1583

←— Concrete

Excerpt from [VDI 1988] Thermal capacity concrete

2-7   We assume that you mean lead in Table 4-9.
We checked the values given in Fig. 59 of [Guruswamy 2000] which we sent you and found that the figure has a wrong scale unit on the y-axis. The correct stress must read (10^2 x 981 Pa).
This can be concluded from values given in Table 30 of [Guruswamy 2000] (see below) for Pb-0.06% Cu for 9.5 hours where a stress value of 8.6 MPa is given. This corresponds for 10 hours in Fig. 59 to a value of approx. 9.8 MPa.
The values used for 10 000 hours and 100 000 hours of 2 MPa and 1.7 MPa were used as very conservative also with respect to the accuracy of reading in Fig. 59.

164   Chapter 2

Table 30 Stress-Rupture Lives of Various Lead Alloys at Room Temperature [168]. (Courtesy of Lead Development Association, London.)

Material	Details of extrusion[a]	Stress-rupture life (h) at a stress of			
		10.3 MPa	8.6 MPa	6.9 MPa	5.2 MPa
Tadanac lead	C		0.75–1.0	4–8	110–116
Tadanac lead	P		2.25	24–28	348–700
Pb–0.06% Cu	P	0.75	9.5	78–100	1,050–1,126
Pb–0.015% Te	C	3.5	21	150–175	1,512
Pb–2% Sn		~160	~400	~950	
Alloy E (0.4% Sn, 0.2% Sb)	C		130	390–440	1,680
Alloy E (0.4% Sn, 0.2% Sb)	R[b]		~500	~1,440	~4,000
Pb–0.4% Sb	200°C	>29 to <93	<261	816	2,784
Pb–0.4% Sb–As	200°C	185	744	3,360	15,165
Pb–1% Sb		~270	~950	~3,000	
Alloy B (0.85% Sb)	C[b]	~800	~1,200	~1,700	~12,000
Alloy B (0.85% Sb)	R[b]	~500	~800	~1,150	~1,400
Pb–0.03% Ca		~2,000			
Alloy F-3 (0.15% As; 0.1% Sn; 0.1% Bi)	160°C		326	4,034	
Alloy F-3 (0.15% As; 0.1% Sn; 0.01% Bi)	200°C		288	5,714	

[a]C = continuous extrusion pressure; temperature of extrusion approx. 250°C; P = pipe pressure; temperature of extrusion 100–120°C; R = commercial Ram pressure; temperature of extrusion approx. 160°C.
[b]5% prestrain before testing.

2-8   In Table 4-48 the mechanical properties of the steel materials are listed for the
        1:3 test model and for the original cask.
        The values for the test model are actual values at room temperature as given in
        the material certificates of the manufacturing documentation.
        The values for the same steel materials can be different because for different
        parts of the model other feed material was used.

        The specified values for the original cask are minimum standard values at 100 °C
        for the materials.
        There is a writing error in Table 4-48 in the last column. The values listed for the
        ultimate strength R_m are not for 100 °C but for room temperature because only
        these values are specified in the standards, so the column header should read Rm
        at RT.

        Taking this into regard there is no discrepancy to the values given in Tables 4-5,
        4-8 and 4-11.

2-9   The density of the Helium is by a factor of 2 lower because according to Handling
        Instruction PA-02-06 Rev. 2 Annex 1 the pressure in the cask is adjusted to 0.5
        bar.

        For the specific heat capacity of the "Zirconium zones" the value for aluminum
        was used which is besides Zircaloy and steel an optional cladding material.
        Aluminum has the highest specific heat capacity of these materials.
        For the steady-state calculations the heat capacity has no influence. For the
        transient calculations of the fire accident a high heat capacity of the inner
        materials means that the temperature of the content will be a little lower but the
        temperature of the outer lead layer which is the critical material will be a little
        higher:
        Nevertheless the influence of the assumed heat capacity is very small.

        As stated in the SAR the specific heat capacity of Balsa wood is taken from
        [Niemz]. According to this literature the heat capacity of wood is nearly
        independent from the raw density, but dependent from the moisture content. The
        value of 1700 J/kg K corresponds to a moisture content of 12% (see diagram of
        specific heat capacity in dependence of the moisture content from [Niemz] below).
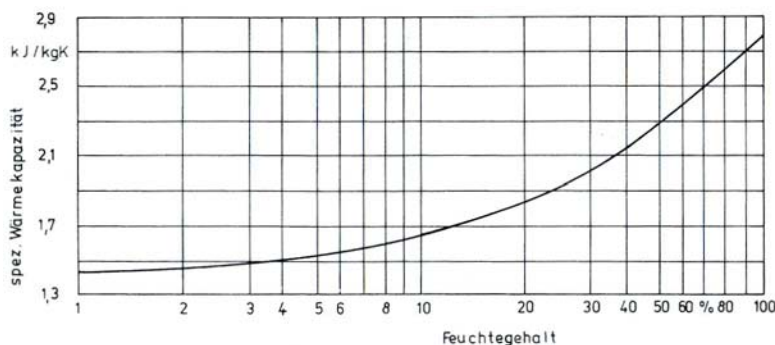
2-10   See answer to 4-4

2-11   The construction, design and drawings of the cans are described in Specification
        SB-09-01 Rev. 2 and the inspection is described in Test Procedure PA-09-08

Rev. 0. A translation of both documents will be submitted separately to this document. They will be officially included in licensing documentation in the next revision of the Certificate of Approval.

2-12   The assumptions for the release radioactive material are given in chapter 6.3.2. There it is distinguished between fuel rods with burn-up up to 33 GWd/MgHM, fuel rods with burn-up between 33 GWd/MgHM and 62 GWd/MgHM and fuel with burn-up above 62 GWd/MgHM. Especially chapter 6.3.2.2.2 deals with fuel rods between 33 GWd/MgHM and 62 GWd/MgHM. These assumptions are evaluated positive by BAM in their Examination Report (chapter 5.3).

Containment

3-1   The designation Helium 4.6 specifies a Helium purity with the following composition:
He ≥ 99.996 vol%; O_2 ≤ 5 vpm; N_2 ≤ 20 vpm; H_2O ≤ 5 vpm; CH ≤ 1 vpm; Ne ≤ 10 vpm.
The designation Helium 4.6, Helium 5.0 etc. is not standardized but a German industrial agreed designation system with specified purities. The first figure specifies the number of "nines", the second figure after the dot the first digit different from "nine".

Shielding

4-1   A translation of all sketches SK020503-1E to SK020503-7E will be separately included to the submittal of this document. In addition a new sketch SK020503-9E is included which gives the dimensions of the transport container. The width of the container is also the width of the transport vehicle.

4-2   In section 7.7.3 factors for consideration of the source height are determined for the surface of the package, 1 m distance from the package and 2 m distance from the vehicle. These factors take into account that for the same total source strength the dose resulting from sources extending over the whole packaging length is smaller than for concentrated small sources. The concept of considering the source length is also applied for the thermal analysis.

In tables 7-31 and 7-34 it is shown that the determined factors used in the specified equations guaranteed that the dose limits for the surface of the package and for a distance of 2 m from the vehicle are met.

The factors for consideration of the source length are specified in the certificate of package approval and have to be observed for compliance with the certificate.

4-3   Fuel rods shorter than the cavity length are fixed with steel spacers. For shorter fuel rods with an active length less than the maximum length (443.5 cm) the correction formulas for the dose rates for shorter sources apply (see question 4-2).

E. g., if the source has a length of 100 cm, then the correction formula given in Table 2 of the certificate (= Table 7-20 of chapter 7 of the SAR) would give penalty factors of

Surface of the package:

$f_{\gamma,OF}$ (100cm) = 1.0 + 18*exp(-0.015 * 100) = 5

2 m distance from the vehicle:

$f_{\gamma,2m}$ (100cm) = 1.8 – 0.0018 * 100) = 1.62

Hence, the gamma dose rate expected for a short source of 100 cm would be for the same total gamma source strength by a factor of 5 higher for the surface of the package and by a factor of 1.62 higher in 2 m distance from the vehicle.

4-4   Pellets and pellet scraps will always be loaded into the packaging by using closed cans. These cans will be positioned by steel spacers inside the cavity. The NCS 45 is not equipped to receive loose pellets or pellet scrap. However, for the containment analysis these cans are considered to be non-existent as no specified leakage rate was tested. Welded cans have a certain level of quality assurance and are leak tested.

4-5   Tables 1.5 and 1.5a in the certificate of package approval comply with Table 2-6 and Table 2.6-1 of chapter 2 "Description of contents" on which the SAR is based. Table 10 in Section 3.5 of the Design Examination Certificate of BAM contain writing errors which have been corrected by the BfS (German competent authority) in the certificate. We would like to remind you that mechanical and thermal issues are checked in Germany by BAM and shielding and criticality issues (which are affected by the writing errors) by BfS. We will point out these inconsistencies to BAM. We are not authorized to make any changes to the BAM paper.

4-6   Based on own calculations the German competent authority changed the correction factor for neutrons for 2 m distance from the vehicle slightly to have a more conservative factor. We will change the concerned table in the next revision of chapter 7 to be consistent with the certificate.

4-7   The package NCS 45 is designed for some 40 different contents covering UOX MOX, MTR, FBR, graphite based and other special fuel. In Revision 0 of the certificate only UOX fuel with contents 1.1 to 1.5 and structural material was considered. Including all design contents in the first issue of the certificate would have caused considerable delays. However, all calculations for the design contents are available. Some contents using special internal arrangements (neutron shielding) resulted in higher weighing factors for some gamma energy groups. In order to provide consistency with respect to these factors for all future revisions of the certificate it was agreed by the German competent authority to use covering factors valid for all design contents.

The differences affect only Tables 7-19 and 7-28. Tables 7-20 and 7-21 are not affected as these tables give only relative dose rates for the variation of the source length.

The weighing factors given in Table 7-19 are especially for small gamma energies smaller than the factors given in Table 7-28, which is conservative, the weighing factors given in Table 1 of the certificate comply mostly with Table-28, some values were rounded by the German competent authority.

4-8   For the determination of the dose rates on the surface and in 2 m distance from the vehicle the formulas given on page 2 of the certificate of package approval are

relevant. The gamma and neutron source term of the fuel to be transported must be known, measured or calculated, as appropriate. With the formulas it is checked that the dose rates are to be expected within the allowable limits. Stainless steel cladding with eventually a gamma contribution due to e. g. Co-60 will contribute to the gamma source term of the fuel and will be considered automatically.

The permissible heavy metal masses defined for the various contents (e. g. Table 1.1a etc.) are limits which were defined in the containment analysis (see chapter 6 of the SAR). These heavy metal masses assure only that the activity release is below the required limits. Dose rate limits are met if the equations on page 2 of the certificate are fulfilled.

4-9   The source spectra in Table 7-7 and 7-8 are used to calculate the dose rate profiles in section 7.9. In section 7.9 it is shown where the maximal dose rates are to be expected. These calculations show as well the ratio between radial and axial dose rates. A typical source was selected to provide realistic dose rate profiles useful for the mentioned assessment.

For Table 7-19 individual calculations for each gamma energy group were carried out (see the explanation in Section 7.7.2). The results of these calculations are given in Table 7-18. Here the assumed source strength for each energy group as well as the result and statistics are documented. Table 7-19 is then based on Table-7-18.

Table 7-19 and finally the amended Table 7-28 (see question 4-7) are valid for all source spectra as with the weighing factors (individually determined and valid only for the NCS 45 packaging) each source spectrum is normalized to an energy group of 2.0 to 2.5 MeV.

4-10   See answer to question 4-9

4-11   The permissible heavy metal mass for undamaged fuel rods and canned fuel is derived in Chapter 6 "Containment" of the SAR

Criticality

5-1   The "Guide to Verification and validation of the SCALE-4 Criticality Safety Software can be found on the Web http://www.ornl.gov/sci/scale/pubs/tm12834.pdf, which is a report listed under SCALE Validation & Benchmarks.

Page 44 (submitted separately) of the SCALE 5 Notebook available on the Web specifies that the Guide is also applicable to future versions of SCALE.

Criticality Safety Validation Input Files can be found on the WEB under http://www.ornl.gov/sci/scale/download_validation.htm. All these benchmarks have been recalculated and checked against the original results. No significant deviations were found.

5-2   The methodology used for the proof for content 1.2 is based on the methodology used for the proof for content 1.1 with an additional "layer" of variational calculations.

For each of the fissile material distributions listed in Table 8-8 of the SAR the same variational calculations as for content 1.1 have been carried out. I. e., for

content 1.2 in total 14 variational calculations starting with a most compact active zone to a most expanded zone (18 cm diameter) have been carried out.

For the most reactive case (26.2983 g/cm fissile material, water fraction 0.7966) the individual calculation is documented below in Table 1, Figure 1 and Figure 2.

So the fissile material distribution is varied between 5.4156 g/cm and 61.3038 g/cm active length and for each of these distributions the water fraction is varied from 0.0931 – which is for model HET1 always the most compact arrangement of the fuel rods in the smallest possible active diameter – up to the maximum possible water fraction which is reached when the array of fuel rods is fully expanded within the bounding 18 cm diameter.

Table 1:   *Calculation results model HET1, Uranium oxide fuel, enrichment 5.3 wt% U-235, 26.2983 g U-235 / cm, max. 18 cm fissile diameter*

Modelled fissile material	Active diameter	Lattice spacing	Water fraction	k_{eff}	σ	gen. skip
g/cm	cm	cm	g/cm³	-	-	-
26.2278	8.57741	0.0986	0.0931	0.4770	0.0016	7
26.2278	9.54236	0.1098	0.2690	0.5240	0.0015	3
26.2356	10.93538	0.1260	0.4448	0.5978	0.0017	33
26.2278	11.91114	0.1374	0.5328	0.6562	0.0020	4
26.2435	13.20902	0.1524	0.6207	0.7244	0.0017	7
26.2278	14.04199	0.1621	0.6647	0.7686	0.0018	4
26.2278	15.05698	0.1739	0.7086	0.8173	0.0020	3
26.2356	15.65532	0.1809	0.7306	0.8373	0.0018	10
26.2905	16.33172	0.1888	0.7526	0.8720	0.0017	3
26.2513	16.70478	0.1931	0.7636	0.8839	0.0019	3
26.2983	17.10480	0.1977	0.7746	0.9021	0.0017	3
26.2826	17.31596	0.2002	0.7801	0.9100	0.0017	3
26.2983	17.53519	0.2028	0.7856	0.9161	0.0019	5
26.2983	17.64799	0.2041	0.7883	0.9183	0.0019	3
26.2826	17.76301	0.2054	0.7911	0.9243	0.0017	7
26.2826	17.82137	0.2061	0.7924	0.9252	0.0021	30
26.2983	17.88032	0.2068	0.7938	0.9258	0.0019	3
26.2826	17.91001	0.2071	0.7945	0.9286	0.0018	7
26.2513	17.93986	0.2075	0.7952	0.9299	0.0019	3
26.2435	17.95484	0.2076	0.7955	0.9304	0.0020	3
26.2826	17.96985	0.2078	0.7959	0.9292	0.0017	6

Modelled fissile material	Active diameter	Lattice spacing	Water fraction	k_{eff}	σ	gen. skip
g/cm	cm	cm	g/cm³	-	-	-
26.2983	17.97738	0.2079	0.7960	0.9267	0.0021	3
26.2983	17.98491	0.2080	0.7962	0.9319	0.0022	3
26.2983	17.99245	0.2081	0.7964	0.9319	0.0017	3
26.2983	18.00000	0.2082	0.7966	0.9338	0.0019	20

Figure 1:   *k_{eff} as function of water fraction, calculation model HET1, Uranium oxide fuel, enrichment 5.3 wt% U-235, 26.2983 g U-235 / cm, max. 18 cm fissile diameter*
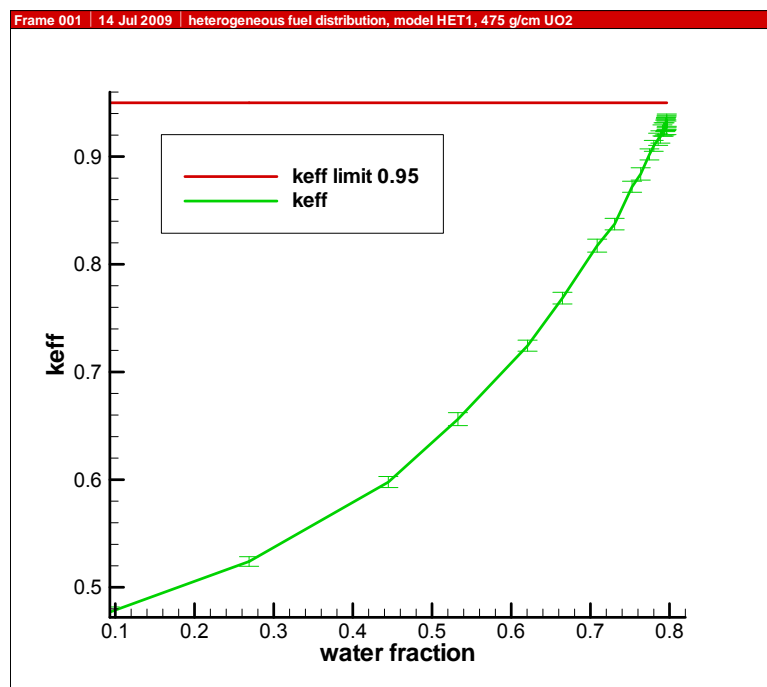
error bar = 3 σ

Figure 2:   *k$_{eff}$ as function of active diameter, calculation model HET1, Uranium oxide fuel, enrichment 5.3 wt% U-235, 26.2983 g U-235 / cm, max. 18 cm fissile diameter*
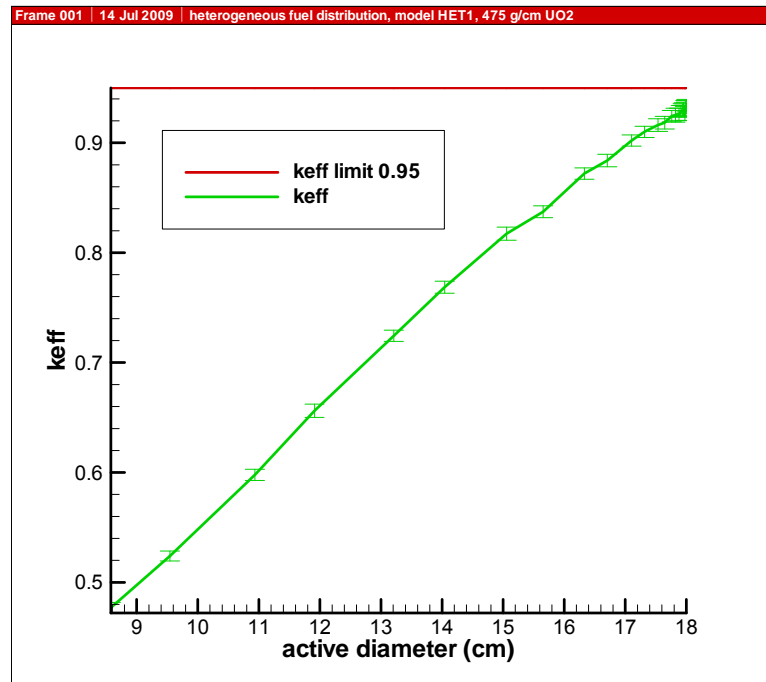
error bar = 3 σ

5-3   The methodology used for the proof for content 1.3 is based on the methodology used for the proof for content 1.1 with an additional "layer" of variational calculations (see also answer to question 5-2).

For each considered height listed in Table 8-9 of the SAR the same variational calculations as for content 1.1 have been carried out. With the given maximum total fissile mass of 1380 g for each fissile material height a fissile material distribution can be determined which is listed in column 3 of Table 8-9. For each height, i. e. for each of the resulting fissile material distribution an individual variational calculation is carried out. Hence, for content 1.3 in total 19 variational calculations each starting with a most compact active zone to a most expanded zone (22 cm diameter equal to cavity diameter) have been carried out.

For the most reactive case (fissile height 52 cm, 26.5464 g/cm fissile material, water fraction 0.8624) the individual calculation is documented below in Table 2, Figure 3 and Figure 4.

So the fissile material distribution is varied between 13.6198 g/cm (for a fissile height of 100 cm) and 46.3197 g/cm active length (for a fissile height of 30 cm) and for each of these distributions the water fraction is varied from 0.0931 – which is for model HET3 always the most compact arrangement of the fuel rods in the smallest possible active diameter – up to the maximum possible water fraction which is reached when the array of fuel rods is fully expanded within the bounding 22 cm diameter of the cavity.

Table 2:   *Calculation results model HET3, Uranium oxide fuel, enrichment 5.3 wt% U-235, 26.5464 g U-235 / cm, fissile height 52 cm, max. fissile diameter equal to cavity diameter*

Modelled fissile material	Active diameter	Lattice spacing	Water fraction	k_{eff}	σ	gen. skip
g/cm	cm	cm	g/cm³	-	-	-
26,5464	8,6293	0,0992	0,0931	0,4491	0,0014	20
26,5464	9,7090	0,1117	0,2854	0,5026	0,0015	8
26,5781	10,4292	0,1201	0,3816	0,5389	0,0018	72
26,5464	11,3401	0,1307	0,4778	0,5845	0,0022	3
26,5781	11,8963	0,1372	0,5258	0,6160	0,0017	5
26,5464	12,5442	0,1447	0,5739	0,6479	0,0016	3
26,5622	13,3120	0,1536	0,6220	0,6880	0,0017	3
26,5464	14,2421	0,1645	0,6701	0,7276	0,0018	9
26,5781	14,7874	0,1708	0,6941	0,7540	0,0019	3
26,5701	15,4011	0,1779	0,7182	0,7770	0,0022	15
26,5464	16,0987	0,1860	0,7422	0,8018	0,0018	4
26,6018	16,9014	0,1954	0,7663	0,8372	0,0020	3
26,6018	17,8384	0,2063	0,7903	0,8627	0,0022	3
26,6177	18,3698	0,2124	0,8023	0,8762	0,0016	4
26,6018	18,9520	0,2192	0,8143	0,8944	0,0025	3
26,6177	19,5936	0,2267	0,8264	0,9082	0,0021	3
26,5701	20,3056	0,2350	0,8384	0,9205	0,0018	6
26,6177	20,6921	0,2395	0,8444	0,9288	0,0060	3
26,6177	21,1017	0,2442	0,8504	0,9310	0,0018	6
26,5781	21,3159	0,2467	0,8534	0,9330	0,0020	3
26,6177	21,5367	0,2493	0,8564	0,9324	0,0018	6
26,6098	21,6498	0,2506	0,8579	0,9355	0,0018	31
26,6177	21,7647	0,2519	0,8594	0,9336	0,0018	7
26,5781	21,8228	0,2526	0,8602	0,9346	0,0017	3
26,6177	21,8814	0,2533	0,8609	0,9371	0,0019	3
26,6177	21,9109	0,2536	0,8613	0,9359	0,0019	5
26,6177	21,9404	0,2540	0,8617	0,9365	0,0019	3
26,6177	21,9702	0,2543	0,8620	0,9404	0,0022	5
26,5464	22,0000	0,2547	0,8624	0,9406	0,0019	3

Figure 3:   *k_{eff} as function of water fraction, calculation model HET3, Uranium oxide fuel, enrichment 5.3 wt% U-235, 26.5464 g U-235 / cm, fissile height 52 cm, max. fissile diameter equal to cavity diameter*
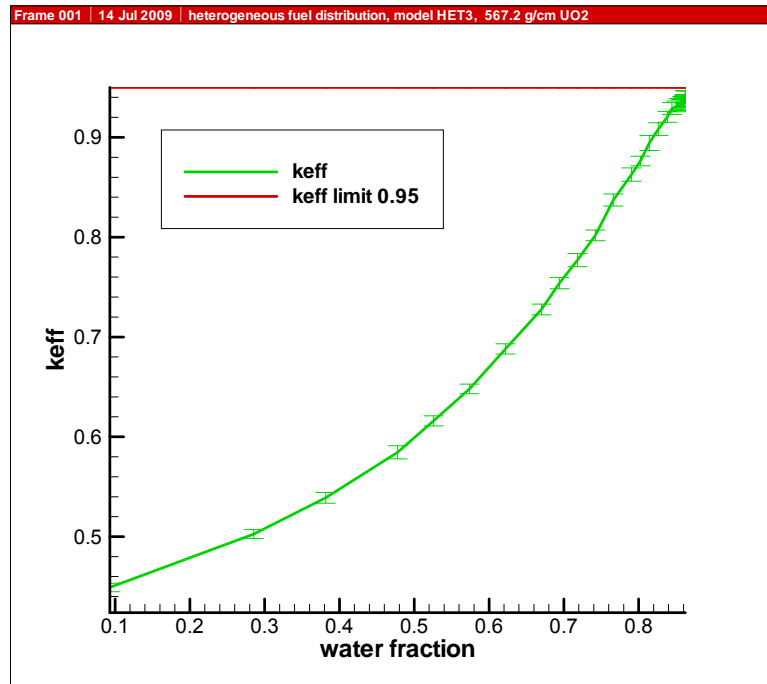
error bar = 3 σ

Figure 4:   *k_{eff} as function of active diameter, calculation model HET1, Uranium oxide fuel, enrichment 5.3 wt% U-235, 26.5464 g U-235 / cm, fissile height 52 cm, max. fissile diameter equal to cavity diameter*
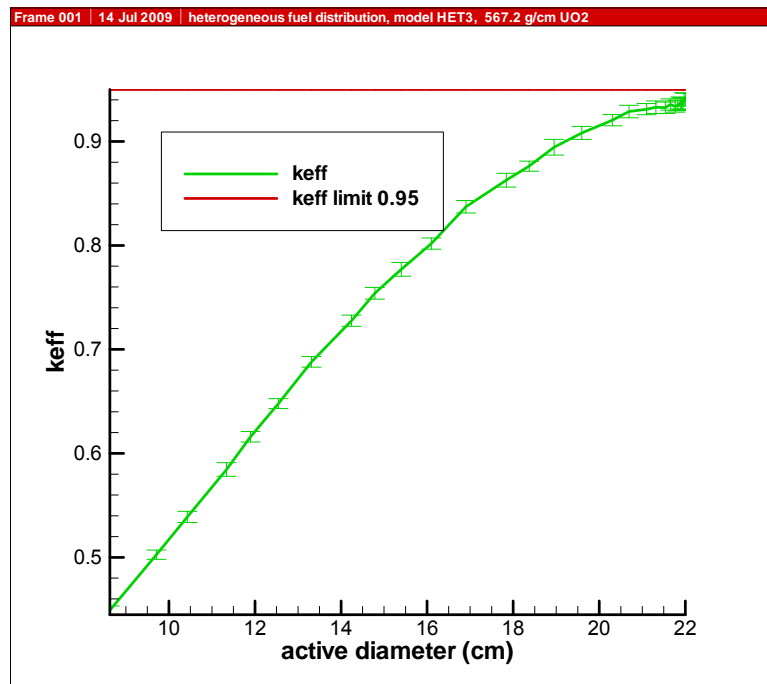
error bar = 3 σ

5-4   Please read fissile material radius as title of the second column of Table 8-9

5-5   Please see the details explained in answer to question 5-3.

5-6   The methodology used for the proof for content 1.4 in Section 8.6.1.4 is the same as used for content 1.2 (please see also the answer to question 5-2), however for content 1.4 the bounding diameter is the cavity diameter and for content 1.2 the bounding diameter is the centering frame tube with 18 cm diameter. Here like for content 1.2 the proof is based on the methodology used for the proof for content 1.1 with an additional "layer" of variational calculations.

For each of the fissile material distributions listed in Table 8-10 of the SAR the same variational calculations as for content 1.1 have been carried out. I. e., for content 1.4 in total 19 variational calculations starting with a most compact active zone to a most expanded zone (22 cm diameter) have been carried out.

For the most reactive case (28.1236 g/cm fissile material, water fraction 0.76996) the individual calculation is documented below in Table 3, Figure 5 and Figure 6.

So the fissile material distribution is varied between 13.9308 g/cm and 52.9901 g/cm active length and for each of these distributions the water fraction is varied from 0.0931 – which is for model HET1 always the most compact arrangement of the fuel rods in the smallest possible active diameter – up to the maximum possible water fraction which is reached when the array of fuel rods is fully expanded within the bounding 22 cm diameter.

Table 3:   Calculation results model HET1, Uranium oxide fuel, enrichment 3.4 wt% U-235, 28.1236 g U-235 / cm, max. fissile diameter equals cavity diameter

Modelled fissile material	Active diameter	Lattice spacing	Water fraction	k_{eff}	σ	gen. skip
g/cm	cm	cm	g/cm³	-	-	-
28,1236	11,1316	0,0985	0,0931	0,5108	0,0015	46
28,0890	12,3315	0,1092	0,2623	0,5646	0,0014	3
28,1236	13,0997	0,1161	0,3469	0,6053	0,0016	3
28,1038	14,0334	0,1244	0,4315	0,6546	0,0019	3
28,1137	14,5826	0,1293	0,4738	0,6852	0,0016	3
28,1236	15,2023	0,1349	0,5161	0,7156	0,0015	3
28,1236	15,9091	0,1412	0,5584	0,7471	0,0016	5
28,0841	16,7253	0,1485	0,6007	0,7843	0,0018	21
28,1038	17,6826	0,1570	0,6430	0,8255	0,0017	3
28,1236	18,2277	0,1619	0,6641	0,8417	0,0017	8
28,1236	18,8269	0,1672	0,6853	0,8682	0,0017	3

Modelled fissile material	Active diameter	Lattice spacing	Water fraction	k_{eff}	σ	gen. skip
g/cm	cm	cm	g/cm³	-	-	-
28,0890	19,4897	0,1731	0,7064	0,8860	0,0018	7
28,1137	20,2282	0,1797	0,7276	0,9030	0,0017	3
28,1236	20,6306	0,1833	0,7381	0,9113	0,0015	3
28,0940	21,0582	0,1871	0,7487	0,9205	0,0016	6
28,0989	21,2822	0,1891	0,7540	0,9285	0,0016	3
28,1137	21,5136	0,1912	0,7593	0,9291	0,0016	7
28,1236	21,6321	0,1923	0,7619	0,9326	0,0017	3
28,1137	21,7527	0,1933	0,7646	0,9340	0,0021	8
28,1137	21,8137	0,1939	0,7659	0,9314	0,0017	4
28,1137	21,8753	0,1944	0,7672	0,9337	0,0015	3
28,1088	21,9374	0,1950	0,7685	0,9333	0,0018	6
28,1236	22,0000	0,1955	0,7699	0,9372	0,0020	3

Figure 5:   *k_{eff} as function of water fraction, calculation model HET1, Uranium oxide fuel, enrichment 3.4 wt% U-235, 28.1236 g U-235 / cm, max. fissile diameter equals cavity diameter*
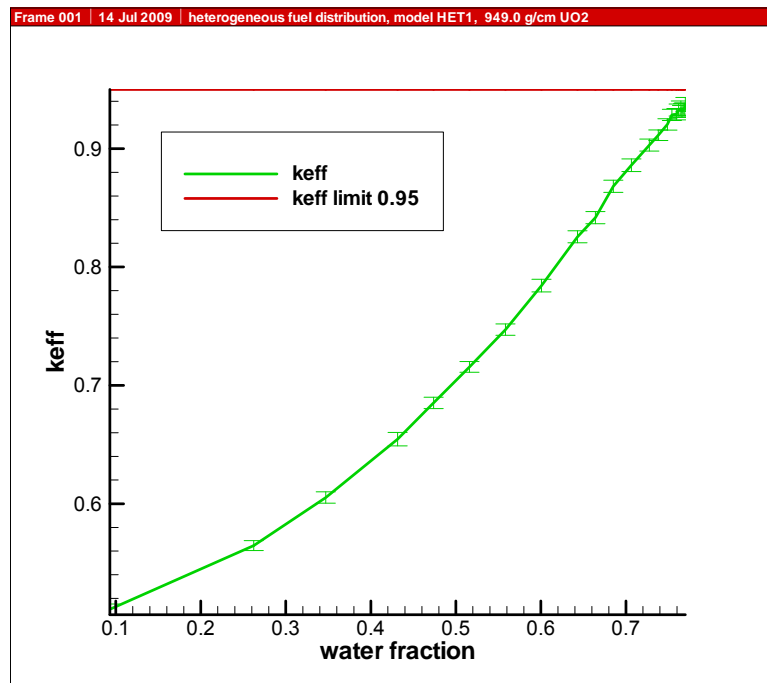
error bar = 3 σ

Figure 6:   *k$_{eff}$ as function of active diameter, calculation model HET1,
Uranium oxide fuel, enrichment 3.4 wt% U-235, 28.1236 g U-235
/ cm, max. fissile diameter equals cavity diameter*
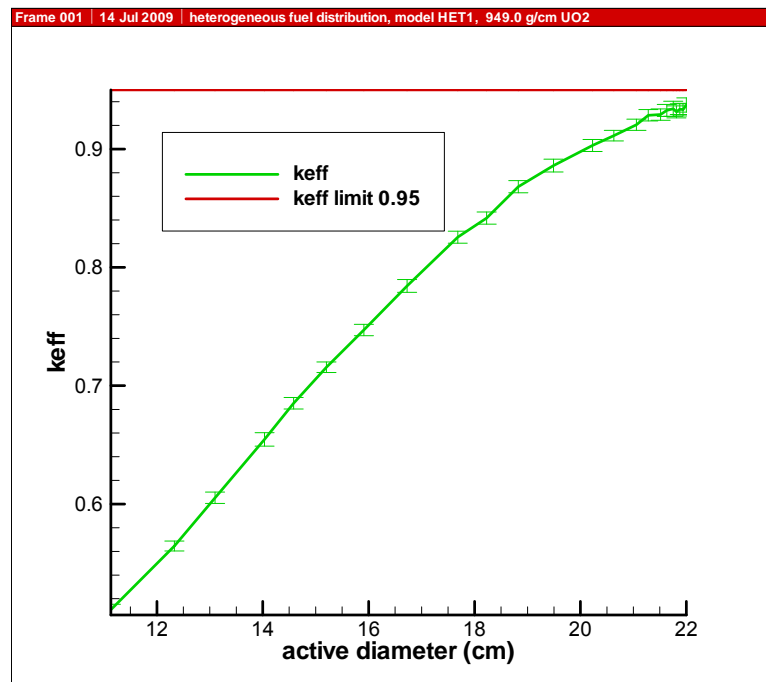
error bar = 3 σ

5-7   The methodology used for the proof for content 1.5 in Section 8.6.1.5 is the same
as used for content 1.2, 1.3 and 1.4 (please see also the answer to question for
these contents). For content 1.5 the bounding diameter is the cavity diameter as
for content 1.4. Here like for content 1.2, 1.3 and 1.4 the proof is based on the
methodology used for the proof for content 1.1 with an additional "layer" of
variational calculations.

For content 1.5 the model HET4 deviating from the models used for contents 1.1
to 1.4 is used. On one hand model HET4 is close to the design of the centering
frames shown in drawings no. 0-090-108-00-00 and 0-090-112-00-00, on the
other hand with model HET1 a smaller number of guiding tubes and hence fuel
than with model HET4 could be modeled.

For each of the fissile material distributions listed in Table 8-11 of the SAR the
same variational calculations as for content 1.1 have been carried out. I. e., for
content 1.5 in total 14 variational calculations starting with a most compact active
zone to a most expanded zone (22 cm diameter) have been carried out.

For the most reactive case (69.7 g/cm fissile material, water fraction 0.6199) the
individual calculation is documented below in Table 4, Figure 7 and Figure 8.

So the fissile material distribution is varied between 36.6 g/cm and 121.9 g/cm
active length and for each of these distributions the water fraction is varied from
the smallest possible value – which depends for model HET4 on the specific
configuration for the smallest possible active diameter – up to the maximum

possible water fraction which is reached when the array of fuel rods is fully
expanded within the bounding 22 cm diameter.

Table 4:   *Calculation results model HET1, Uranium oxide fuel, enrichment
7.0 wt% U-235, 69.7 g U-235 / cm, max. fissile diameter equals
cavity diameter*

Modelled fissile material	Active diameter	Lattice spacing	Water fraction	k_{eff}	σ	gen. skip
g/cm	cm	cm	g/cm³	-	-	-
69,6993	15,6133	2,0200	0,2454	0,7027	0,0017	3
69,6993	16,5408	2,1400	0,3276	0,7529	0,0017	3
69,6993	17,8875	2,3142	0,4251	0,8221	0,0017	9
69,6993	18,6971	2,4190	0,4738	0,8569	0,0014	3
69,6993	19,6277	2,5394	0,5225	0,8885	0,0016	3
69,6993	20,1483	2,6067	0,5468	0,9076	0,0016	5
69,6993	20,7126	2,6797	0,5712	0,9238	0,0017	3
69,6993	21,0132	2,7186	0,5834	0,9257	0,0017	5
69,6993	21,3272	2,7593	0,5956	0,9352	0,0018	3
69,6993	21,4896	2,7803	0,6016	0,9371	0,0019	3
69,6993	21,6558	2,8018	0,6077	0,9385	0,0016	4
69,6993	21,7403	2,8127	0,6108	0,9403	0,0018	3
69,6993	21,8259	2,8238	0,6138	0,9409	0,0019	33
69,6993	21,9124	2,8350	0,6169	0,9376	0,0017	5
69,6993	22,0000	2,8463	0,6199	0,9414	0,0019	62

Figure 7:   *k$_{eff}$ as function of water fraction, calculation model HET1, Uranium oxide fuel, enrichment 7.0 wt% U-235, 69.7 g U-235 / cm, max. fissile diameter equals cavity diameter*
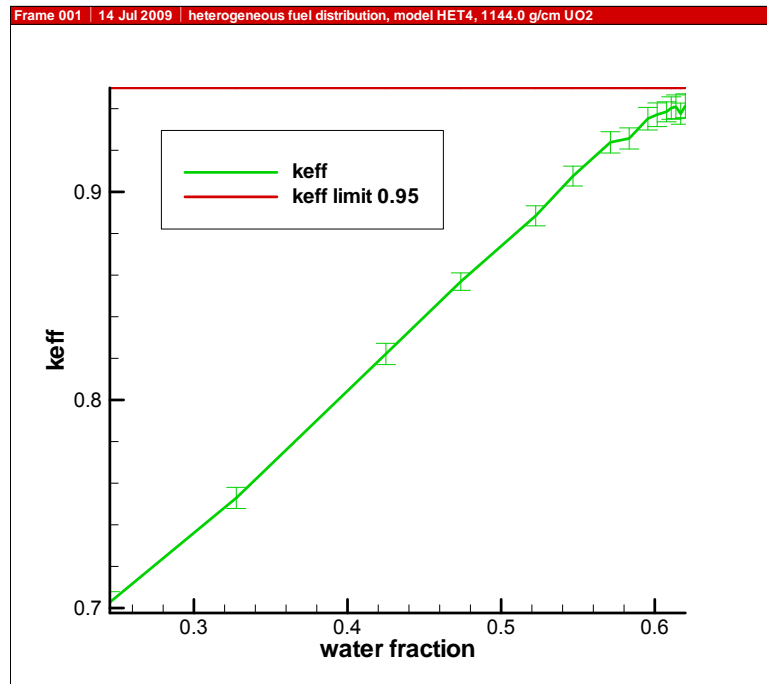
error bar = 3 σ

Figure 8:   *k$_{eff}$ as function of active diameter, calculation model HET1, Uranium oxide fuel, enrichment 7.0 wt% U-235, 69.7 g U-235 / cm, max. fissile diameter equals cavity diameter*
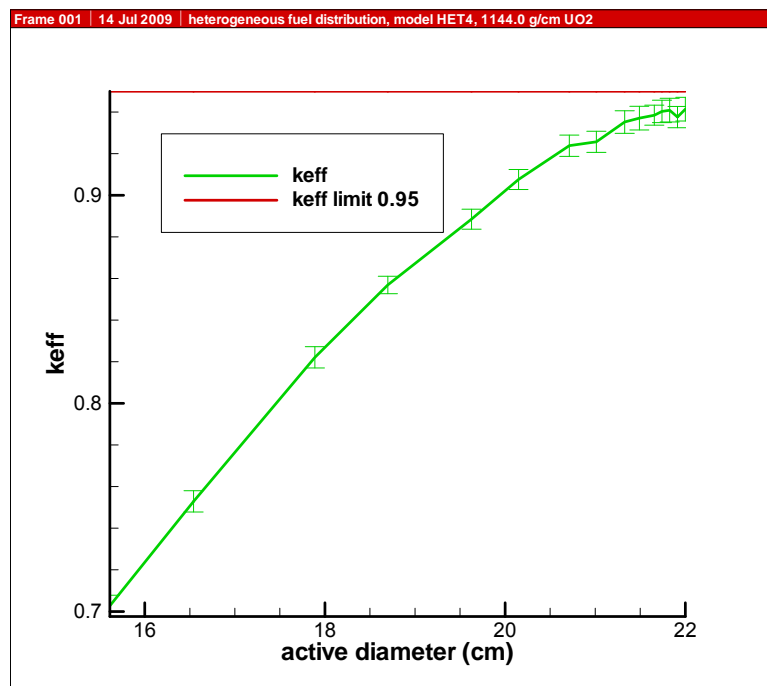

error bar = 3 σ

In the following details of the models used for the calculations are given. In the following figures fuel is always red, the guiding tubes are light yellow, the inner cavity wall is yellow, lead is green and water in the cavity is cyan.

The calculations start with the smallest investigated fissile mass distribution of 36.99 g/cm[1] which complies with a UO_2 mass distribution of 600 g/cm. The smallest number of guiding tubes which can accommodate this fuel mass is 27, the diameter of the fuel is 1.6068 cm. Figure 9 shows the most compact configuration possible, Figure 10 a intermediate configuration and Figure 11 the most expanded configuration with the outer guiding tubes touching the cavity wall.

Figure 9:   Calculation model HET4, configuration with 27 fuel rods, most compact configuration

---
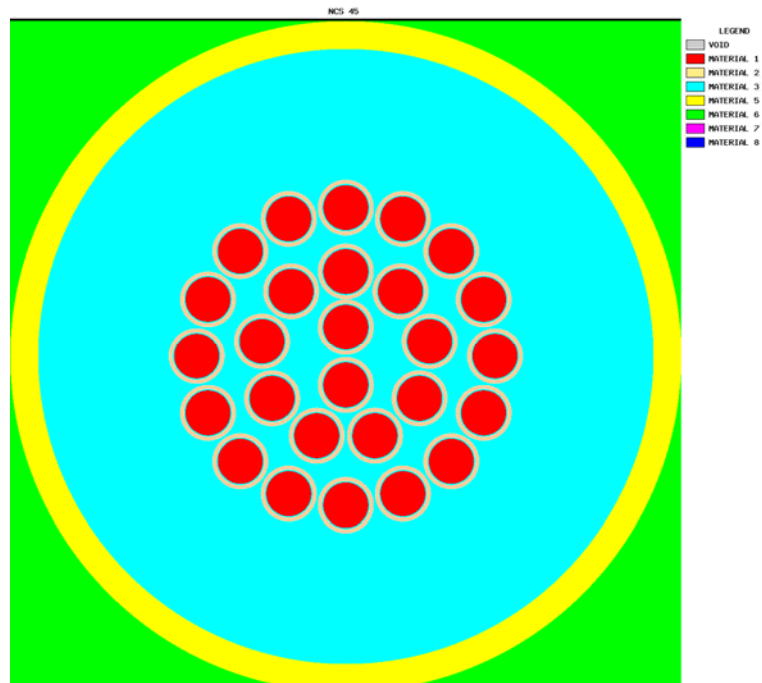
[1] Remark: the fissile material distribution listed in Table 8-11 of the SAR was calculated with a UO_2 density of 10.8 g/cm^3, the calculations were performed with the theoretical density of 10.96 g/cm^3

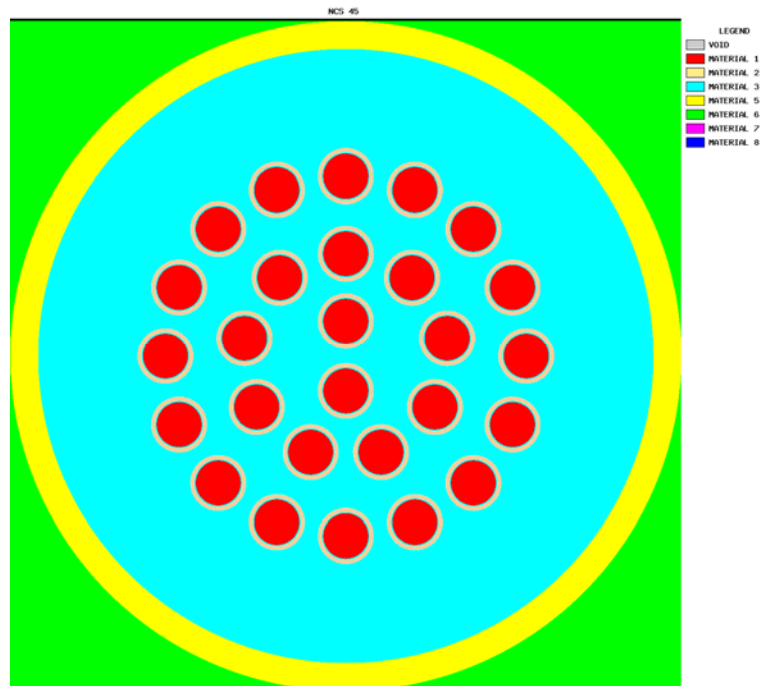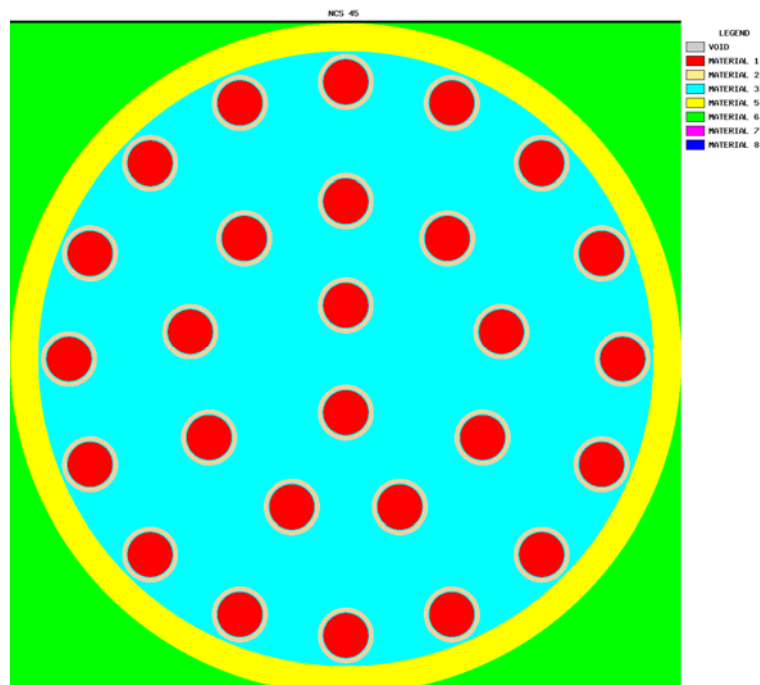Figure 10:   *Calculation model HET4, configuration with 27 fuel rods, intermediate configuration*

Figure 11:   *Calculation model HET4, configuration with 27 fuel rods, most expanded configuration*

The UO$_2$ mass distribution is increased by steps of 100 g/cm and the smallest number of guiding tubes calculated which could accommodate that fuel. For a fissile mass of 67.81 g/cm and a UO$_2$ mass distribution of 1100 g/cm 46 guiding tubes are required. The diameter of the fuel is 1.666 cm. Figure 9 shows the most

compact configuration possible, Figure 10 a intermediate configuration and
Figure 11 the most expanded configuration with the outer guiding tubes touching
the cavity wall.

Figure 12:   *Calculation model HET4, configuration with 46 fuel rods, most
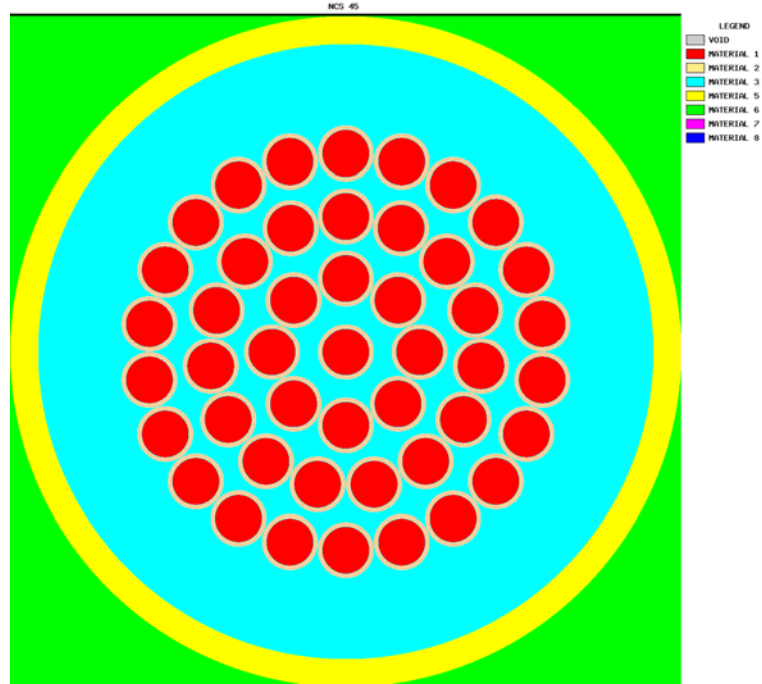compact configuration*

Figure 13:   *Calculation model HET4, configuration with 46 fuel rods,
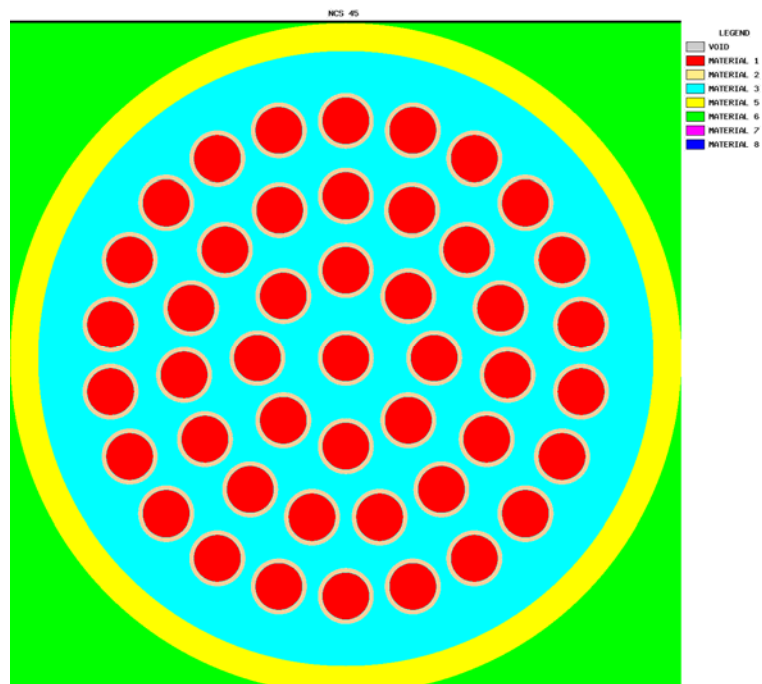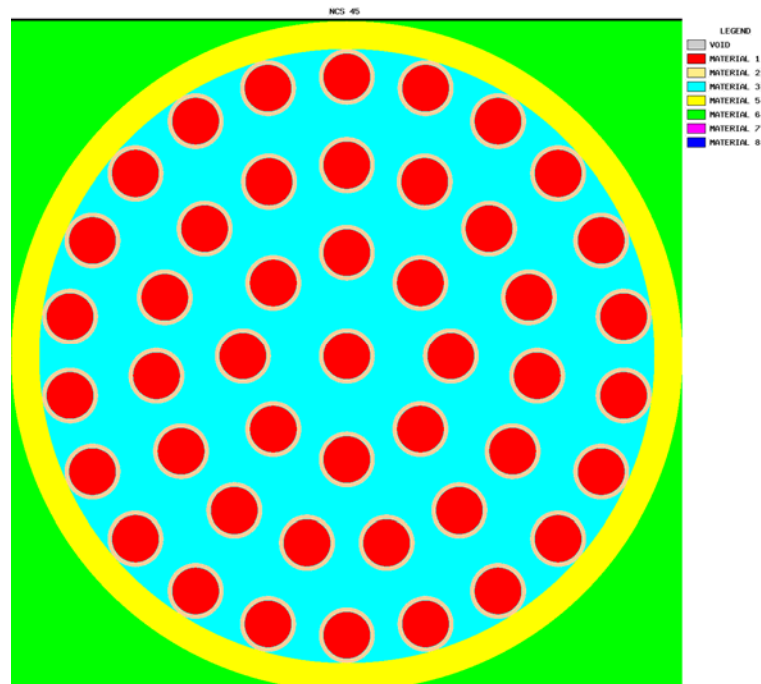intermediate configuration*

Figure 14:   *Calculation model HET4, configuration with 46 fuel rods, most expanded configuration*

Maximal reactivities are reached for 43 fuel rods with a UO_2 mass distribution of 1000 g/cm (fissile mass distribution 61.65 g/cm), 46 fuel rods with a UO_2 mass distribution of 1100 g/cm (fissile mass distribution 67.81 g/cm), and 50 fuel rods with a UO_2 mass distribution of 1200 g/cm (fissile mass distribution 73.98 g/cm) with a steep decrease of the reactivity for smaller and larger fissile mass distributions (see Fig. 8-12 of the SAR).

Subsequently the influence of the fuel diameter on reactivity was investigated.

First, for 46 guiding tubes the maximum amount of fissile material distribution was investigated, UO_2 mass distribution of 1144 g/cm (fissile mass distribution 70.52 g/cm), fuel rod diameter 1.7 cm. The maximal reactivity was reached for the most expanded configuration with $k_{eff} = 0.9414$.

Next for 50 guiding tubes a UO_2 mass distribution of 1150 g/cm (fissile mass distribution 70.89 g/cm), fuel rod diameter 1.63 cm was investigated. Maximal reactivity was reached also for the most expanded configuration with $k_{eff} = 0.9253$, which is significantly less (8 to 10 standard deviations) than for the configuration of 46 fuel rods with 1,7 cm fuel rod diameter.

For 50 guiding tubes with a UO_2 mass distribution of 1243 g/cm (fissile mass distribution 73.98 g/cm), fuel rod diameter 1.67 cm the maximal reactivity was also reached for the most expanded configuration with $k_{eff} = 0.9348$.

Next for 50 guiding tubes a UO_2 mass distribution of 1150 g/cm (fissile mass distribution 76.63 g/cm), fuel rod diameter 1.7 cm was investigated. Maximal

reactivity was reached also for the most expanded configuration with k_{eff} = 0.9385.

Finally, the same calculations were carried out for 43 guiding tubes with fuel rods with a diameter of 1.7 cm. The maximal reactivity was also reached for the most expanded configuration with k_{eff} = 0.9404.

The conclusion is that

- Maximal reactivity is reached in all cases for fuel rods with a diameter of 1.7 cm filling the guiding tube completely

- Maximal reactivity is reached for a range of 43 to 50 guiding tubes with the aforesaid fuel rods

- Maximal reactivity is reached for the most expanded configuration when the outer row of fuel rods touches the inner cavity wall.

It has to be remarked that the calculation model is very conservative. The cladding of the fuel rods is completely neglected, which would restrict the possible diameter of the fuel. Furthermore, practical considerations like the necessary gap between guiding tube and fuel to load the fuel rods have been neglected completely.

5-8   The contamination values in footnote 1 in Tables 6 and 7 of the Design Examination Certificate (also Tables 2-2-1 et sec. in the SAR) are surface contamination values of PWR fuel rods.
BWR fuel rods normally have a higher surface contamination as PWR rods. The activity release calculations for PWR and BWR fuel rods are both based on the surface contamination values of PWR fuel rods in footnote 1. Therefore if it can be proven that the surface contamination of BWR fuel rods is less or equal to the values for PWR fuel rods (footnote 1) the specified mass of HM according to the values with footnote 1 are allowed. If the surface contamination of BWR fuel rods exceeds these values the allowable mass of HM has to be reduced according to footnote 2.

5-9   Enclosed please find calculation note RN-09-06 Rev. 0 taking into account a conservatively estimated amount of water in the package during accident conditions of transport.

The density of water between the packages in the array of packages was varied, please see Table 8-16 of the SAR. Row 1 of the results shows a water filled distance between the packages, row 2 a distance of 2 cm, row 3 a distance of 0 cm, but still the gusset between the packages flooded, and row 4 finally shows the results for an infinite array of packages without any water between the packages.

Row 5 finally shows the reactivity of a fissile material distribution of 130.5 g/cm taking into account a complete loss of water out of the thermal insulation. This leads to maximal reactivity.

In calculation note RN-09-06 Rev. 0 the assumption of a fissile material distribution of 130.5 g/cm is compared to the licensed contents 1.1 to 1.5. Additionally, water from various sources (damaged fuel rods, remaining water

after drying, water ingress during the immersion test) is evaluated and criticality analyses are carried out taking into account the evaluated amount of water.

Operation Procedures, Acceptance Criteria and Maintenance Tests

6-1   The Trunnion screws and threads are checked completely after manufacture and periodically in accordance with Test Procedure No. WP-02-02.
In this procedure a load test (step 16) is required according to Test Procedure No. PA-02-04.
This load test also includes the inspection of the three highest stressed screws/threads plus two additional random chosen screws/threads before and after the load test according to Test Instruction No. PA-02-05 Rev. 2, Chapter 9.3.